Plasmonic effect of annealed gold islands for improving the efficiency of organic solar cells

Marco Notarianni, Kristy Vernon, Alison Chou, Jinzhang Liu, Nunzio Motta*

Institute of Future Environments and School of Chemistry, Physics, and Mechanical Engineering,

Queensland University of Technology, Brisbane QLD 4001, Australia

Embedding metallic nanoparticles in organic solar cells can enhance the photoabsorption through light trapping processes. This paper investigates how gold islands obtained by annealing 3-10 nm thick Au layers affect the photoabsorption. Using finite-difference time-domain simulations, the cell efficiency for various island geometries and thicknesses are analyzed and the properties of the islands for maximal photocurrent are discussed. It is shown that a careful choice of size and concentration of gold islands could contribute to enhance the power conversion efficiencies when compared to standard organic solar cell devices. The conclusions are then compared to experimental data for thermally annealed gold islands in bulk heterojunction solar cells. The results of this paper will contribute to the optimisation of plasmonic organic solar cell systems and will pave the way for the development of highly efficient organic solar cell devices.

Keywords: Organic Solar Cells, Bulk Heterojuncion, Plasmonic, Metallic Nanoparticles, Gold,

1. INTRODUCTION

There has been much research interest into organic solar cells (OSCs) as they have the potential to be cheaper than their conventional silicon counterparts [1, 2]. However three pitfalls of these devices still need to be solved: (i) the power conversion efficiency (PCE) [3]; (ii) the device lifetime [4]; and (iii) the large scale production [5].

In recent years, much effort has been directed at increasing the photon absorption into OSCs. In fact, the active layer thickness of these devices is usually limited to ~100 nm because of the low carrier mobilities of the conducting polymer [6] and the short lifetime of the excitons [7]; this limits the number of photons that can be absorbed, thereby reducing substantially the efficiency. For this

reason, increasing the light absorption would help to increase the power conversion efficiency. It has been demonstrated that the PCE can be increased dramatically by increasing the optical path length of the light in the device[8]. Light trapping to increase the optical path length has already been studied extensively for thin film silicon solar cells but not much work has been done for organic solar cells. Research on light trapping in silicon solar cells has been focused on the use of metallic nanoparticles, with studies directed at obtaining the optimal particle shape, size and filling factor [9-13]. However, much of this research has been based on the use of nanoparticles with defined geometry.

This research discusses the use of gold (Au) islands in organic solar cells for increasing the PCE, comparing for the first time experimental results on cell efficiency to a theoretical model based on the actual microscopic structure of the Au islands. It is well known that the shape and coverage of Au islands on a substrate changes dramatically with small increases of film thickness. Our islands have not a regular shape, so it is not possible to use standard models based on simple shapes. By importing SEM images of the islands into finite-difference time-domain models we have been able to model the effects of light trapping in a real island distribution, and to discuss how random gold geometries affect the PCE. The results of the finite-difference time-domain models are then compared to experimental values of PCE we obtain by depositing and annealing a gold film as part of an organic solar cell. The findings of this investigation are not only helpful for organic solar cells but for silicon solar cells as well.

2. METHOD

Several gold island morphologies were grown on ITO/glass electrodes by sputtering gold followed by thermal annealing (Fig. 1a). The organic solar cell was then built on top of these substrates by spin coating 20 nm of PEDOT:PSS and 100 nm of P3HT:$PC_{71}BM$, respectively. The solar cell structure was completed by evaporating 80 nm of Al as back contact (Fig. 1b). Further details of the fabrication can be found in [14]. A solar cell without gold on the ITO electrode was also fabricated as a standard.

Gold layers of 5 nm, 3 nm, 1 nm and 1 nm through a mask (a 10x10 array of 1 mm diameter holes spaced 1 mm), were deposited on ITO and annealed at 300°C in Ar atmosphere in order to avoid an increase of the sheet resistance of the ITO due to a reaction with oxygen [15]. SEM images of the gold islands formed on ITO are shown in Fig. 2 (a-d), along with the statistical distribution the area, obtained by analyzing images with a total area $\mathbf{A_{total}}$ given in table 2. As the thickness decreases the shapes become less irregular and more spherical, Fig. 2 (c) and (d). The coverage of the Au islands also changes with thickness. As expected, the annealing of the 5 nm gold layer results in more gold coverage while the 3 nm gold film exhibits larger islands and less film coverage. For 1 nm gold film, small particles with round shapes similar to hemispheres are obtained. For the 1 nm layer the resulting particles are very compact with a smaller distance between individual particles compared to the 3 nm and 5 nm case. For the 1 nm Au film evaporated through the mask, the spacing between the particles is wider, so more light is expected to be scattered into the device.

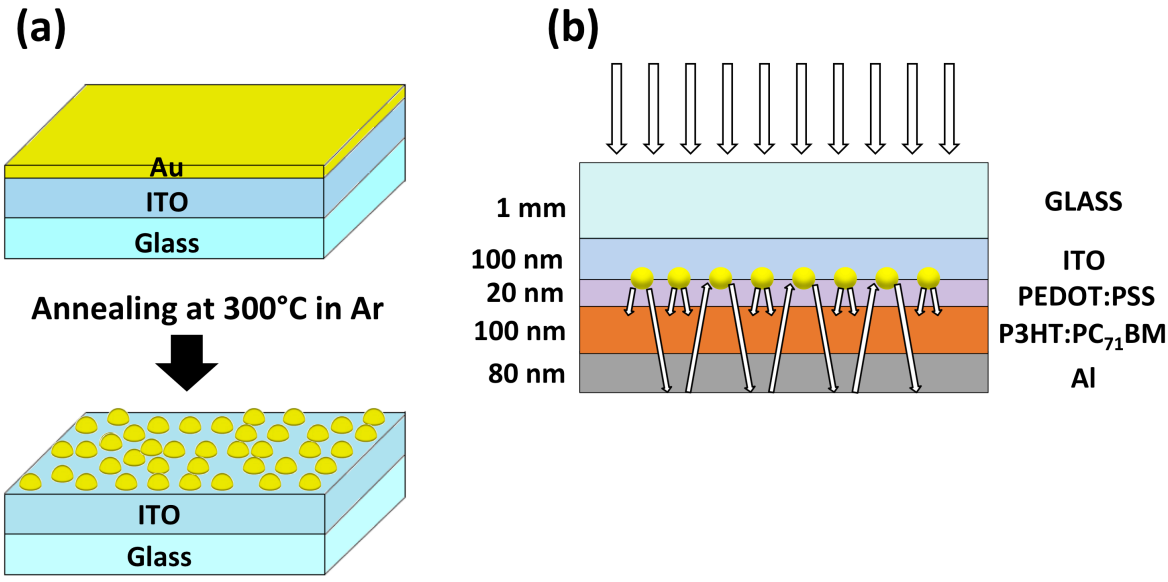

Fig. 1. (a) Schematic of the gold islands formed after annealing on the ITO electrode. (b) Organic solar cell schematic.

In order to accurately calculate the height of the gold islands we analysed SEM images of adequate size with the software Image J [16]. Knowing the area of the particles ($A_{islands}$), the total area of the image analysed (A_{total}) and the thickness of the Au film sputtered before annealing (h_{film}), we were able to calculate the average height of the particles ($h_{islands}$) with the formula:

$$A_{total} \cdot h_{film} = A_{islands} \cdot h_{islands} \qquad (1)$$

The calculated average height of the particles after annealing is 13.8 nm, 8.8 nm and 3.05 nm for the 5 nm, 3 nm, 1 nm Au gold film deposited on ITO respectively. When the evaporation occurs through a mask the equivalent height of the particles increases to 4.73 nm, overestimated because of the presence of the mask. Table I summarizes all the parameters extracted from the SEM images in order to calculate the average height of the Au islands.

Table I. Average height of the islands as obtained from the SEM images and formula (1) on a total area $\mathbf{A_{total}}$ as indicated in column 2.

h_{film} (nm)	A_{total} (μm^2)	$A_{islands}$ (μm^2)	$h_{islands}$ (nm)
5 nm	23.15	8.38	13.82
3 nm	24.44	8.26	8.88
1 nm	6.25	2.05	3.05
1 nm + mask	25.92	5.49	4.73

We also analysed the area distribution of a statistical sample of the islands (Table II), which confirms the shrinking of the average island size with the decreasing of the thickness (Fig. 2). The average area of an island is respectively 2873.17 nm^2 for 5 nm deposition, 980.24 for 3 nm and 205.66 nm^2 for 1 nm. The calculated equivalent radius, (assuming all the islands as circular) is 30, 17 and 8.09 nm, respectively.

Table II. Statistical analysis of the islands obtained by depositing decreasing Au thickness.

Thickness (nm)	Number of islands	Island Average Area (nm^2)	Equivalent Radius (nm)	Islands/μm^2	Area fraction
5	2916	2873.17	30.24	125.98	0.36
3	8430	980.24	17.66	344.91	0.34
1	9965	205.66	8.09	1593.76	0.33
1 + mask	13293	412.78	11.46	512.80	0.21

The average area of the islands deposited through the mask raises instead to 412.78 nm^2 and their equivalent radius to 11.46 nm, indicating a coalescence effect. The area fraction is steadily decreasing from 0.36 (5nm) to 0.21 (1 nm + mask). A net 36% drop in the area fraction is noticeable when the islands are deposited through the mask, indicating the effectiveness of the mask in reducing the coverage.

Pillai et al. [11] grew silver islands on a silicon solar cell with a similar procedure and annealing conditions but they were able to achieve a better distribution of the islands on the substrate with a larger distance between each island. The ITO electrode has a roughness of about 3 nm [17], larger than a conventional Si substrate, and so the gold has a difficulty to coalesce to form islands[18, 19]. Island nucleation and ripening in fact is related to the diffusion of the atoms on the surface, which is strongly dependent on the roughness [20].

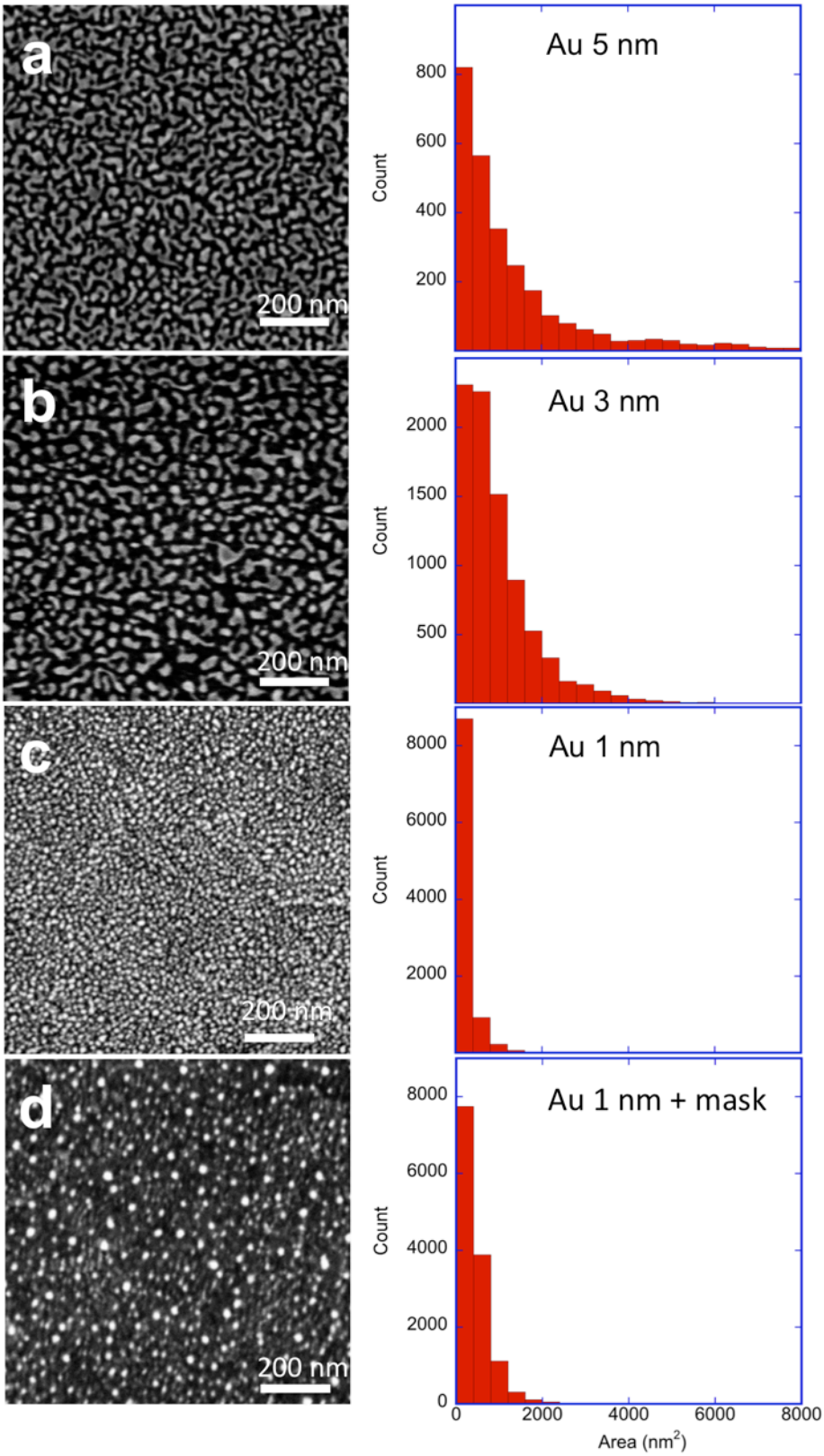

Fig. 2. SEM images and area distributions of the Au islands (details in table I and II) grown on ITO by annealing gold films of (a) 5 nm, (b) 3 nm, (c) 1 nm and (d) 1 nm through a mask (as explained in the text).

The coverage of the Au islands on the ITO substrate and film thickness are important parameters in the performance of the organic solar cell [8]. The light trapping in ultrathin gold films is difficult to model due to the random geometries of the Au islands. To obtain an accurate simulation we employed Lumerical FDTD solutions and imported SEM images of the islands into the software. We then compared the scattering into the PEDOT:PSS layer to the scattering into the PEDOT:PSS layer in the absence of Au films. The wavelength range of 400-700 nm was chosen as it corresponds to the absorption range of the P3HT that is the active material in the device.

A SiO_2 glass substrate with permittivity from Palik et al. [21] a 100 nm layer of ITO with permittivity from Suhr [22], a 20 nm layer of PEDOT:PSS with permittivity from Pettersson et al. [23], 100 nm layer of $PC_{71}BM$:P3HT with permittivity from Li et al. [24] , and finally a 80 nm layer of Al with permittivity from Palik et al. [21] were used for the FDTD simulations. The gold SEM images have been imported and placed on top of the ITO, with the gold permittivity calculated from the Drude model modified to fit with the Johnson and Christy data for visible wavelengths[25].

The scattering into the $PC_{71}BM$:P3HT was calculated (15 nm above the ITO) and normalized against a solar cell without the gold NPs. A scattering > 1 indicates more photons entering the $PC_{71}BM$:P3HT than in the plain solar cell case (i.e. one without Au NPs).

3. RESULTS AND DISCUSSIONS

We compared the light scattering into the PEDOT:PSS layer for a substrate with and without islands. A normalized scattering of 1 indicates that the scattering efficiency of the Au islands solar cell is equal to that of a conventional cell. A normalized scattering greater than 1 indicates that more photons are scattered because of the islands into the PEDOT:PSS compared to the reference cell.

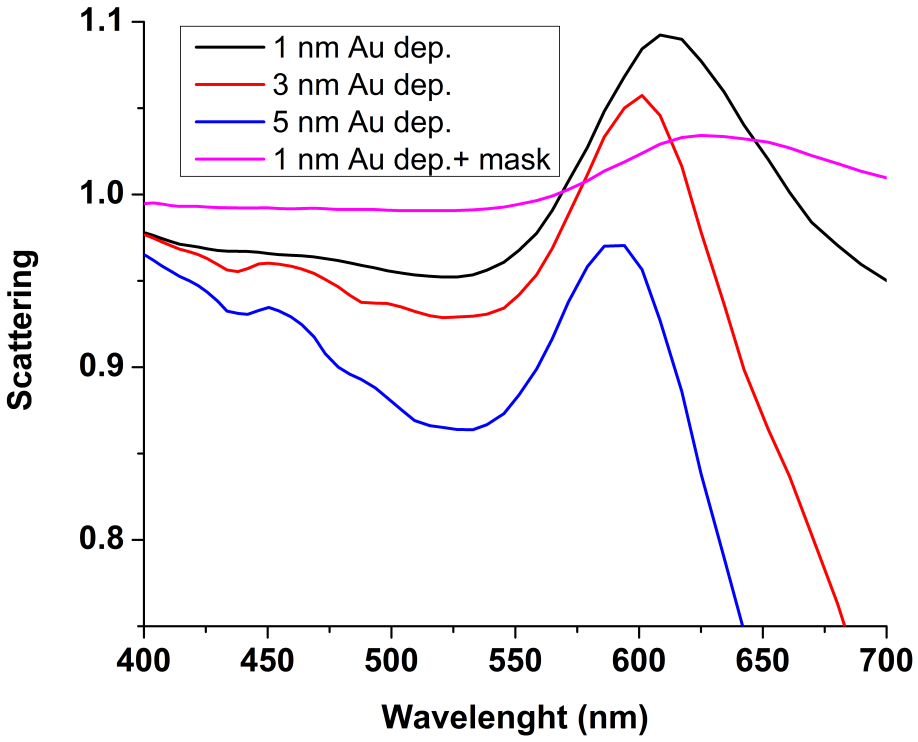

Fig. 3 Normalized scattering into the upper PEDOT:PSS for Au films of 5 nm (black curve), 3 nm (red curve), 1 nm (blue curve) and 1 nm through a mask (purple curve) thickness. The scattering is normalized to the scattering from a cell without Au.

It is clear from Fig. 3 that the 5 nm thick gold layer produces a shadowing effect in the solar cell, as the number of scattered photons into the PEDOT:PSS layer is lower than for the reference cell for all wavelengths considered. Instead, the 3 nm and 1 nm Au thick layers produce a scattering effect larger than 1, i.e. better than in the reference solar cell, for a wide range of wavelengths. The 3 nm thick gold layer produces a scattering larger than 1 in the range 575nm – 620nm, and 570nm - 660nm, respectively. The 1 nm thick Au layer has the maximum overall scattering amplitude, but the efficiency of the solar cell is not as high as expected and it is actually lower than the standard cell (see fig 4).

There are three factors to consider when discussing the scattering behavior of the 1 nm and 3 nm gold layers in solar cells: the gold thickness, the shape of the islands formed and the filling

factor. The 3 nm gold layer leads to increased absorption losses and overall lower scattering amplitude. In fact the islands in this case are large and irregular (average area 980 nm^2), while in the 1 nm case they are small and hemispherical (average area 205 nm^2 , equivalent radius 8.09 nm) (Table II). As shown by Catchpole et al. [10] the best geometry is dipolar, which is obtained in cylindrical and hemispherical particles. This explains why the scattering is higher in the case of the 1 nm gold film, where the particles are hemispherical. However, the losses due to the light reflection at other wavelengths are still significant, limiting the overall efficiency. The 1 nm + mask case shows a smaller peak compared to the other cases but a wider curve indicating reduced overall losses, which compensate for the lower scattering peak. If we plot the normalized scattering vs frequency the the area under the four curves is proportional to 2.83, 3.03, 3.16, 3.22 and for the 5 nm, 3 nm, 1nm, 1 nm + mask respectively, to be compared to 3.21 for bare solar cell (constant scattering = 1). This indicates that more photons scatter into the active layer when the fraction of surface covered by the islands is reduced.

In Fig 4 we present the I-V characteristics obtained in organic solar cells based on the 4 Au island distributions compared to a standard solar cell without Au islands. The best experimental values of the PCE are obtained for the device made with a 1 nm thick gold film evaporated through the mask [26] .

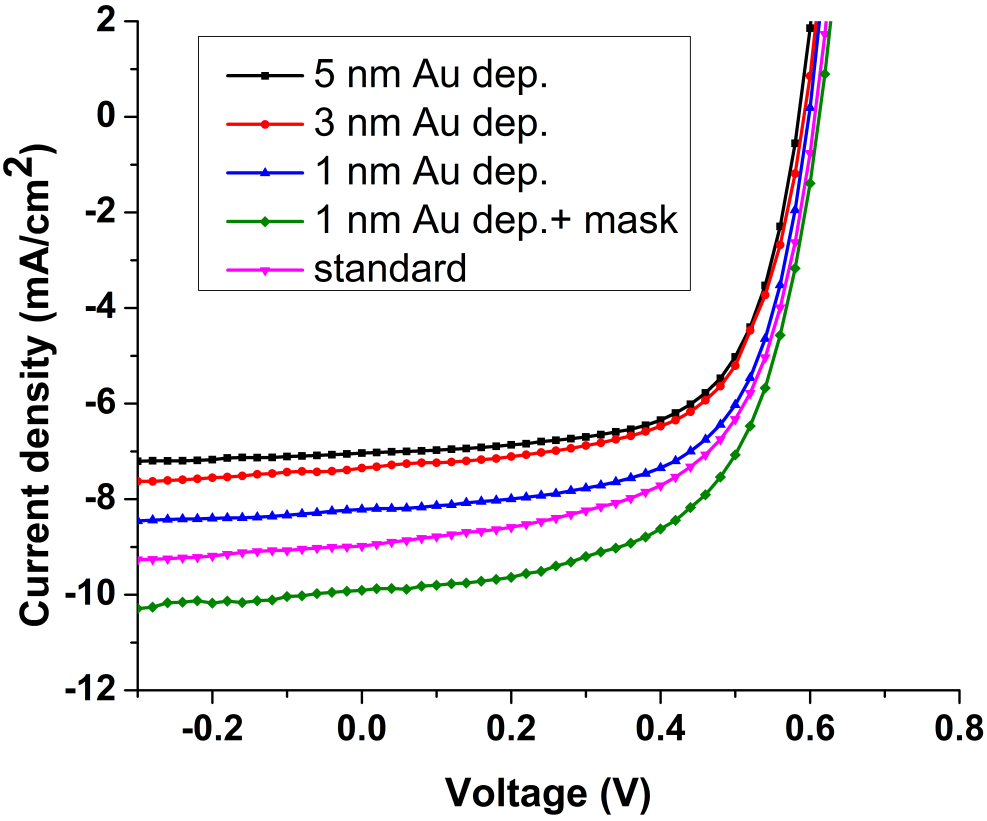

Fig. 4 Current density-voltage characteristics of organic solar cells devices with islands formed by thermal annealing of a Au layer thick 5 nm (black curve), 3 nm (red curve), 1 nm (blue curve), 1 nm through a mask (green curve) and without islands (purple curve).

Table III shows other relevant device parameters of the plasmonic and standard devices e.g. open circuit voltage (V_{oc}), short circuit current density (J_{sc}), fill factor (FF), series resistance (R_s) and power conversion efficiency (PCE).

By comparing these devices, it is possible to appreciate an increase of the PCE due to the reduction of the Au deposited thickness on top of the ITO electrode. As demonstrated by the finite-difference time-domain models and confirmed by the experimental results, the 1 nm thick gold deposition through the mask gives an increased PCE of 10% compared to a standard device because of the hemispherical geometry of the islands obtained, which contribute to an increased light scattering into the device [10] and because of the spacing between the particles[27]. The PCE could be

further increased by finding a balance between the efficiency of the plasmonic structures in the PEDOT:PSS buffer layer and the other components of the solar cell. In fact, it has been demonstrated that a high loading of plasmonic structures can deteriorate the morphology and electrical characteristics of the polymer [28-30]. For this reason, reducing the amount of Au islands on the ITO electrode can be beneficial not only to reduce ohmic losses but also to keep good electrical characteristics of the PEDOT:PSS [14]. Our results indicate that by a further reduction of the amount of Au islands a larger improvement in the solar cell performance can still be achieved[26].

Table III. Electrical characteristics of the devices incorporating Au islands grown on ITO by thermal annealing.

Device	V_{oc} (V)	J_{sc} (mA/cm^2)	R_s (Ω·cm^2)	FF (%)	PCE (%)
NPs, 5 nm Au dep.	0.58	7.03	13.33	65	2.66
NPs, 3 nm Au dep.	0.58	7.34	15.6	64	2.73
NPs, 1 nm Au dep.	0.58	8.21	13.88	65	3.1
NPs, 1nm Au dep.+mask	0.6	9.9	12.53	61	3.64
standard	0.59	8.98	13.14	61	3.26

4. CONCLUSIONS

The plasmonic effect of Au islands in organic solar cells was modeled by numerical methods. The scattering factors are calculated by importing SEM images of the Au island distributions. The results at different coverage demonstrate that it is possible to improve the efficiency by using islands obtained from very thin Au layers, confirming the experimental data. We demonstrate that the particle shape and thickness obtained after annealing Au layers in Ar at 300 ˚C are the key to improve light trapping in organic solar cells and to increase the efficiency. In fact, small hemispherical islands obtained by depositing 1 nm Au layers provide an improvement to the PCE compared to the thicker Au films but still lower when compared to a solar cell without islands. Spacing the particles is another critical parameter to be considered. In fact, we proved that spacing the particles by evaporating and annealing gold through a macroscopic mask is an effective

technique to increase the PCE. We obtained in this way a 10% increase compared to a standard device, because more photons are scattered into the active layer. We explained this result by theoretical simulations based on the real island distribution as obtained by SEM images. Further studies are in progress.

5. ACKNOWLEDGEMENTS

The authors acknowledge the financial support of the Australian Research Council through the Discovery Projects DP130102120 and DP110101454. We also acknowledge the Marie Curie International Research Staff Exchange Scheme Fellowship within the 7th European Community Framework Programme. We thank the technical support of Dr. P. Hines and Dr. H. Diao from the Central Analytical Research Facility of the Institute of Future environments at QUT.

This work was performed in part at the Queensland node of the Australian National Fabrication Facility (ANFF) – a company established under the National Collaborative Research Infrastructure Strategy to provide nano and microfabrication facilities for Australia's researchers.

REFERENCES

1. J. Kalowekamo and E. Baker, *Solar Energy*, 2009, **83**(8), 1224-1231.
2. C. Powell, T. Bender, and Y. Lawryshyn, *Solar Energy*, 2009, **83**(11), 1977-1984.
3. G. Dennler, M. C. Scharber, and C. J. Brabec, *Adv. Mater.*, 2009, **21**(13), 1323-1338.
4. M. Jørgensen, K. Norrman, and F. C. Krebs, *Solar Energy Materials and Solar Cells*, 2008, **92**(7), 686-714.
5. C. J. Brabec and J. R. Durrant, *MRS Bulletin*, 2008, **33**(7), 670-675.
6. R. A. Street, M. Schoendorf, A. Roy, and J. H. Lee, *Physical Review B - Condensed Matter and Materials Physics*, 2010, **81**(20).
7. M. Theander, A. Yartsev, D. Zigmantas, V. Sundström, W. Mammo, M. R. Andersson, and O. Inganäs, *Physical Review B*, 2000, **61**(19), 12957-12963.
8. S. Mokkapati and K. R. Catchpole, *Journal of Applied Physics*, 2012, **112**(10), 101101-101119.
9. S. Mokkapati, F. J. Beck, A. Polman, and K. R. Catchpole, *Applied Physics Letters*, 2009, **95**(5), 053115-053113.
10. K. R. Catchpole and A. Polman, *Applied Physics Letters*, 2008, **93**(19), 191113-191113.
11. S. Pillai, K. R. Catchpole, T. Trupke, and M. A. Green, *Journal of Applied Physics*, 2007, **101**(9), 093105-093108.
12. H. A. Atwater and A. Polman, *Nat. Mater.*, 2010, **9**(3), 205-213.
13. U. Kreibig, Vollmer, M.: 'Optical Properties of Metal Clusters'; 1995, Springer.
14. M. Notarianni, K. Vernon, A. Chou, M. Aljada, J. Liu, and N. Motta, *Solar Energy*, 2013.
15. M. M. Hamasha, T. Dhakal, K. Alzoubi, S. Albahri, A. Qasaimeh, S. Lu, and C. R. Westgate, *IEEE/OSA Journal of Display Technology*, 2012, **8**(7), 383-388.

16. C. A. Schneider, W. S. Rasband, and K. W. Eliceiri, *Nat Meth*, 2012, **9**(7), 671-675.
17. A. M. Rao, A. Jorio, M. A. Pimenta, M. S. S. Dantas, R. Saito, G. Dresselhaus, and M. S. Dresselhaus, *Physical Review Letters*, 2000, **84**(8), 1820.
18. C. E. J. Mitchell, A. Howard, M. Carney, and R. G. Egdell, *Surface Science*, 2001, **490**(1-2), 196-210.
19. J. Siegel, O. Kvítek, P. Slepička, J. Náhlík, J. Heitz, and V. Švorčík, *Nuclear Instruments and Methods in Physics Research Section B: Beam Interactions with Materials and Atoms*, 2012, **272**(0), 193-197.
20. N. Motta, P. D. Szkutnik, M. Tomellini, A. Sgarlata, M. Fanfoni, F. Patella, and A. Balzarotti, *Comptes Rendus Physique*, 2006, **7**(9), 1046-1072.
21. E. D. Palik and G. Ghosh: 'Handbook of optical constants of solids'; 1985, San Diego, Academic Press.
22. B. Shan and K. Cho, *Physical Review B (Condensed Matter and Materials Physics)*, 2006, **73**(8), 081401-081404.
23. L. A. A. Pettersson, S. Ghosh, and O. Inganäs, *Organic Electronics: physics, materials, applications*, 2002, **3**(3-4), 143-148.
24. X. Li, W. C. H. Choy, L. Huo, F. Xie, W. E. I. Sha, B. Ding, X. Guo, Y. Li, J. Hou, J. You, and Y. Yang, *Advanced Materials (Weinheim, Germany)*, 2012, **24**(22), 3046-3052.
25. P. B. Johnson and R. W. Christy, *Physical Review B*, 1972, **6**(12), 4370-4379.
26. M. Notarianni, K. Vernon, A. Chou, M. Aljada, J. Liu, and N. Motta, *Solar Energy*, 2014, **106** 23-37.
27. S. Shahin, P. Gangopadhyay, and R. A. Norwood, *Applied Physics Letters*, 2012, **101**(5), -.
28. X. Li, W. C. H. Choy, H. Lu, W. E. I. Sha, and A. H. P. Ho, *Adv. Funct. Mater.*, 2013, **23**(21), 2728-2735.
29. K. Yao, M. Salvador, C. C. Chueh, X. K. Xin, Y. X. Xu, D. W. Dequilettes, T. Hu, Y. Chen, D. S. Ginger, and A. K. Y. Jen, *Advanced Energy Materials*, 2014, **4**(9).
30. F.-C. Chen, J.-L. Wu, C.-L. Lee, Y. Hong, C.-H. Kuo, and M. H. Huang, *Applied Physics Letters*, 2009, **95**(1), 013305-013303.